Biogeosciences, 22, 55–69, 2025
https://doi.org/10.5194/bg-22-55-2025

Biogeosciences Open Access EGU

A long-term drought reconstruction based on oxygen isotope tree ring data for central and eastern parts of Europe (Romania)

Viorica Nagavciuc[1,2], Gerhard Helle[3], Maria Rădoane[2], Cătălin-Constantin Roibu[2], Mihai-Gabriel Cotos[2], and Monica Ionita[1,2]

[1]Paleoclimate Dynamics, Alfred Wegener Institute for Polar and Marine Research, Bremerhaven 27570, Germany
[2]Forest Biometrics Laboratory – Faculty of Forestry, "Stefan cel Mare" University of Suceava, Universităţii Street No. 13, Suceava 720229, Romania
[3]German Research Centre for Geosciences GFZ, 4.3 Climate Dynamics and Landscape Evolution, Telegrafenberg, Potsdam 14473, Germany

Correspondence: Viorica Nagavciuc (nagavciuc.viorica@gmail.com) and Monica Ionita (monica.ionita@awi.de)

Received: 10 July 2024 – Discussion started: 30 July 2024
Revised: 29 October 2024 – Accepted: 11 November 2024 – Published: 7 January 2025

Abstract. This study investigates the relationship between oxygen isotope ratios (δ^{18}O) in oak tree ring cellulose and past drought variability in Letea Forest, Romania. A δ^{18}O site chronology spanning 1803–2020 was compiled from seven individual time series. δ^{18}O values exhibited a significant negative correlation with moisture-related variables (cloud cover, relative humidity, and precipitation) and a positive correlation with temperature and sunshine duration. This confirms that δ^{18}O from tree rings can be a good proxy for moisture availability. The strongest correlation was found between δ^{18}O and the August Standardized Precipitation Evapotranspiration Index for an accumulation period of 9 months (SPEI9) for central and eastern Europe. This highlights SPEI9 as a superior indicator of drought compared to individual parameters like temperature or precipitation. Using a linear regression model, we reconstructed August SPEI9 variability for the past 200 years. The reconstruction captured interannual and decadal variations, with distinct wet and dry periods. Analysis of large-scale atmospheric circulation patterns revealed a link between high δ^{18}O values (indicating dry conditions) and a high-pressure system over the North Atlantic. Conversely, low δ^{18}O values (indicating wet conditions) corresponded to negative pressure anomalies over Europe. Moreover, extreme values of δ^{18}O are also associated with the prevalence of a hemispheric teleconnection pattern, namely wave number 4. This δ^{18}O chronology and the corresponding August SPEI9 reconstruction offer valuable tools for understanding past climate variability and its relationship with large-scale atmospheric and oceanic circulation patterns.

1 Introduction

Droughts are a recurring natural phenomenon with significant environmental and socio-economic impacts (Kreibich et al., 2022). Understanding past drought occurrences and their frequency, intensity, and spatial extent is crucial for predicting future occurrences, identifying trends, mitigating risk, and adapting water management strategies, particularly as climate change intensifies (Van Loon et al., 2024; IPCC, 2021).

While instrumental records provide valuable insights into recent droughts, they only span a rather short time frame, making it challenging to assess long-term drought variability and identify potential patterns. In this context, tree rings emerge as powerful archives of past environmental conditions, acting as biological data loggers and recording environmental changes in the arboreal system year after year throughout the lifespan of a tree. Analyzing the variations in their width, density, and isotopic compositions provides valuable insights into historical climatic conditions, including temperature, precipitation, and drought variability (Nagavciuc et al., 2020; Schweingruber, 1988; Siegwolf et al., 2022; Leavitt, 2010).

Among the various tree ring proxies, stable oxygen isotopes ($\delta^{18}O$) have proven to be a powerful tool for reconstructing past drought occurrences in very different environments across various climate zones and altitudes (Saurer et al., 2012; Feng et al., 2022; Van der Sleen et al., 2015; Baker et al., 2022; Nagavciuc et al., 2019b, 2024a; Pumijumnong et al., 2020). The $\delta^{18}O$ values in tree ring cellulose reflect the ratio of heavier (^{18}O) to lighter (^{16}O) oxygen isotopes incorporated during cellulose formation. This ratio is primarily influenced by the availability of soil water, making it highly sensitive to drought stress (McCarroll and Loader, 2004; Allen et al., 2019; Gessler et al., 2022; Siegwolf et al., 2022).

Trees primarily take up water from the soil, and this soil water is replenished by precipitation. The isotopic composition of this soil water is influenced by various atmospheric factors, including temperature, precipitation intensity, and humidity (Dansgaard, 1964; Sharp, 2007; Saurer et al., 2012). At the leaf surface, water undergoes evapotranspiration. Lighter oxygen-16 isotopes evaporate more readily, leaving the remaining leaf water enriched in heavier oxygen-18. The degree of enrichment generally depends on the leaf-to-air vapor pressure difference, which is predominantly connected to air temperature and humidity. Additionally, large-scale atmospheric circulation patterns can influence temperature, precipitation, and humidity, indirectly affecting $\delta^{18}O$ in leaf water. Drier conditions enhance this evapotranspiration, further increasing the oxygen-18 concentration of leaf water (Gessler et al., 2014; Roden et al., 2000). Therefore, analyzing the $\delta^{18}O$ values in tree rings provides a direct proxy for past drought events (Gagen et al., 2022; Loader et al., 2020; Young et al., 2015; Freund et al., 2023; McCarroll and Loader, 2004; Nagavciuc et al., 2024a).

The $\delta^{18}O$ values in oak tree ring cellulose have shown a strong correlation with water availability (Robertson et al., 1995; Young et al., 2015). Coupled with the extensive, centuries-long records at an annual resolution and the broad distribution of ancient oak trees, these isotopic values provide a valuable climate proxy, as demonstrated in this study with the Danube Delta, Romania, positioning them as an optimal tool for long-term drought reconstruction beyond conventional climate-sensitive sites. They have the potential to significantly contribute to a better understanding of past drought events beyond the limitations of instrumental data, providing a better picture of past hydroclimatic conditions of the Danube River catchment and integrating over large parts of the country and southeastern and central Europe.

This research aims to reconstruct long-term drought variability over the last 200 years in the southern and eastern parts of Romania using stable oxygen isotopes ($\delta^{18}O$) extracted from oak tree rings from Letea Forest (Romania), Danube Delta (45°18′10″ N, 29°34′51″ E). Romania, located in southeastern Europe, is particularly susceptible to droughts due to its geographical position, which exposes it to a variety of climatic influences, and its complex climate patterns, characterized by seasonal variations, topographic differences, and the impact of atmospheric circulation patterns like the North Atlantic Oscillation and the Eastern Mediterranean Oscillation (Nagavciuc et al., 2022b; Sandu et al., 2008). The country experiences a wide range of climatic conditions, with distinct variations in precipitation patterns across different regions. This inherent variability, coupled with the projected increase in global temperature and altered circulation patterns, raises concerns about the potential for more frequent and intense droughts in the future (Ionita et al., 2021, 2022; Ionita and Nagavciuc, 2021). In a recently report regarding the state of the climate in Romania, it has been shown that, at the country level, there has been a significant increase in the area affected by long-lasting droughts, with exceptional values recorded over the periods 2018–2020 and 2021–2023 (Info Clima, 2024). For example, the longest drought in recent history took place between October 2018 and March 2021, lasting 30 months, and peaked in May 2020. Nevertheless, these finding are subject to a limited temporal evolution (i.e., 1958–2023). In this respect, having long-term drought reconstructions allows us to put the recent events into a longer-term perspective, especially over regions significantly affected by an increase in drought occurrence, like the eastern part of Europe (Ionita and Nagavciuc, 2021). Thus, this study strives to address the following specific objectives: (i) to establish an annually resolved $\delta^{18}O$ chronology compiled from individual sequences from oak trees (*Quercus robur*) sampled in Letea Forest, Danube Delta, Romania; (ii) to develop a robust statistical model linking $\delta^{18}O$ values to instrumental drought indices (Standardized Precipitation Evapotranspiration Index, SPEI), allowing for the reconstruction of past drought variability; (iii) to analyze the spatial and temporal patterns of reconstructed drought occurrences, identifying periods of severe droughts that affected the upstream Danube River catchment; and (iv) to investigate potential linkages between reconstructed drought events and large-scale atmospheric circulation patterns, providing insights into the underlying mechanisms of drought in the region.

2 Methods

2.1 Study site

The Danube Delta has remarkable biodiversity. Being one of the oldest natural reserves in Romania and the northernmost subtropical forest in the world, Letea Forest is a special place with respect to the flora of the Danube Delta (Abdelazim and Diaconu, 2022). Letea Forest is located in the north-eastern part of the Danube Delta, between the Chilia and Sulina arms of the Danube River. Letea Forest (5246.8 ha) has been protected since 1930, and, from 1938 onwards, it was declared a strictly protected area (2825 ha) (Conservarea Pădurii Caraorman). It developed in the form of narrow strips called *hasmacuri*, sometimes several dozen meters long, in the spaces between the sand dunes and is represented by mixed oaks and other broadleaves tree species (e.g., *Quercus*, *Fraxinus*, *Ulmus*), with some very particular elements of species with voluble stems (e.g., *Periploca graeca*, *Vitis sylvestris*, *Humulus lupus*, *Clematis vitalba*) (Pădurea Letea; Conservarea Pădurii Caraorman). The climate is mainly influenced by the proximity of the Black Sea, with warm summers and cold winters. The average annual temperature (i.e., climatological period 1971–2000) at Sulina meteorological station (45°9′13″ N, 29°39′48″ E) (i.e., the closest meteorological station to our sampling site) is around 11.18 °C, with July being the warmest month (∼ 22.16 °C) and January being the coldest one (∼ 0.43 °C). The rainfall is around 278 mm yr^{-1}, with January being the driest month (∼ 15.4 mm $month^{-1}$) and June being the wettest month (∼ 34 mm $month^{-1}$), while the month with the highest relative humidity is December (88.72 %), and the month with the lowest relative humidity is May (78.14 %) (Fig. 1).

2.2 δ^{18}O tree ring chronology

A field campaign in Letea Forest was organized in May 2021, during which 42 increment cores (one core per tree) were extracted using a 5 mm diameter increment borer from 40 living dominant oak trees (*Quercus robur*) with ages between 114 and 396 years, following standard dendrochronological sampling methods (Schweingruber, 1988). All samples were cut using the WSL core microtome (Gärtner and Nievergelt, 2010) and were scanned using a flatbed scanner Epson 11000XL with a true resolution of 1500 DPI. The scanned images were measured using the CooRecorder v.9.31 software, with a precision of 0.01 mm (CDendro and CooRecorder, 2010, http://www.cybis.se/forfun/dendro/index.htm, last access: 20 February 2024). The obtained time series were cross-dated using CDendro (CDendro and CooRecorder, 2010, http://www.cybis.se/forfun/dendro/index.htm, last access: 20 February 2024) and checked for the missing rings using COFECHA software (Holmes, 1983).

The stable isotope analyses were performed for the 1803–2020 period. Latewood rings of seven selected cores were dissected manually with a scalpel to obtain an annual resolution before conducting measurements of each ring individually (no pooling). Holocellulose was extracted from latewood using the Jayme–Wise two-step base-acid methodology and setup as described by Helle et al. (2022): sodium hydroxide (5 % (w/v), 2 × 2 h at 80 °C) for the dissolution of most hemicelluloses and the breakdown of lignins, followed by acidified sodium chlorite (7.5 % (w/v), pH ≈ 4 (acetic acid), 4 × 10 h at 80 °C) to finally eliminate lignins and extractives (Rinne et al., 2005). After extraction, samples were washed thoroughly with Milli-Q water, homogenized (ultrasonic sonde device for Eppendorf sample vials), and freeze-dried for 48 h (Laumer et al., 2009). The resultant homogenized cellulose was weighed (160–200 µg) and packed in silver capsules for stable oxygen isotope analysis. Measurements were completed on an Isotope Ratio Mass Spectrometer Delta V, Thermo Fisher Scientific, Bremen, Germany, with a TC/EA high temperature (HT) pyrolysis device at 1400 °C. The samples analyzed are referenced to standard materials from the International Atomic Energy Agency (IAEA-C3, IAEA-CH6, IAEA-601, and IAEA-602) and checked with secondary standards from Sigma-Aldrich Chemie GmbH, Munich, Germany (Sigma alpha-Cellulose and Sigma Sucrose) using a two-point normalization method (Paul et al., 2007). Sample replication resulted in a reproducibility of better than ±0.3 ‰ for the δ^{18}O values. All isotope values are reported in per mil (‰) relative to the Vienna Standard Mean Ocean Water (VSMOW) (Coplen, 1994) using the traditional δ (delta) notation. The final δ^{18}O chronology was calculated as the arithmetic mean of the multiple measurements.

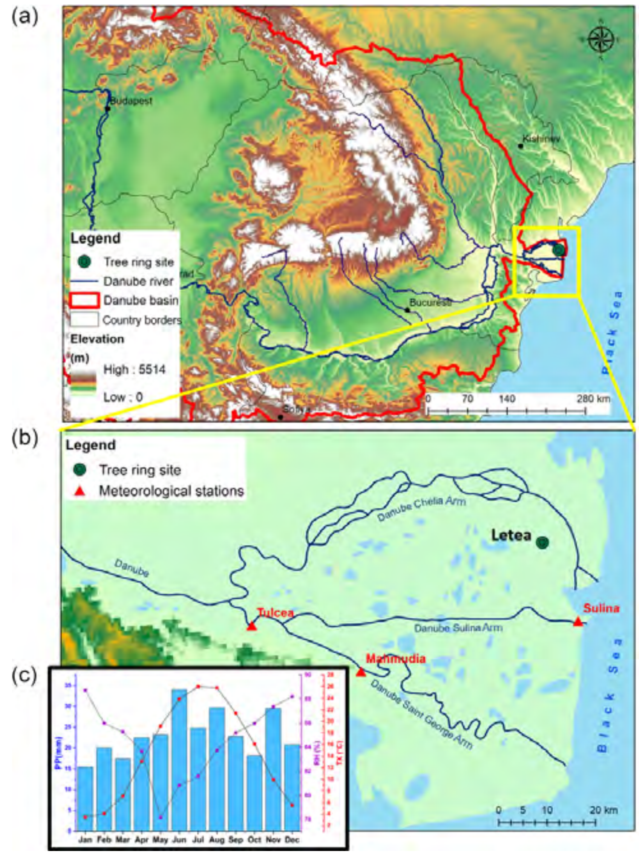

Figure 1. Location of the investigation area: the topographic map of Romania showing the sampling site and the eastern Danube River catchment (red line) **(a)**; the local map of the Danube Delta with locations of the sampling site (green circle) and climate stations (red triangles) **(b)**. Panel **(c)** represents the annual variation in the maximum temperature (red dots), precipitation (PP, blue bars), and relative humidity (violet dots) over the 1971–2000 period at the Sulina meteorological station located ca. 15 km south of the study site.

2.3 Hydroclimate data and $\delta^{18}O$ relationship

The hydroclimatic sensitivity of the $\delta^{18}O$ was tested by performing correlation analyses between $\delta^{18}O$ and precipitation, mean temperature, maximum temperature, relative humidity, cloud cover, and sunshine duration using monthly climate data from the Sulina meteorological station. All correlation analyses were performed from January to December but also for March, April, and May (MAM); June, July, and August (JJA); and January to August (J–A).

Since the available data from Sulina were constrained to 1961–2013, we performed additional analyses with gridded data obtained from the CRU TS v. 4.04 dataset (Harris et al., 2020), covering the period 1901–2020. Given that the stable oxygen isotopes in tree ring cellulose are sensitive to precipitation and temperature, we also tested the relationship with the drought index, namely with the Standardized Precipitation Evapotranspiration Index (SPEI). To compute the SPEI, we used the gridded monthly precipitation (PP), monthly mean air temperature (TT), and potential evapotranspiration (PET). PET is computed using the Penman–Monteith method (Penman, 1948). The correlation between $\delta^{18}O$ chronology and the SPEI index was tested for different timescales, specifically 1 month (SPEI1), 3 months (SPEI3), 6 months (SPEI6), 9 months (SPEI9), and 12 months (SPEI12), and for different months, from January until September of the current year, in order to identify the most suitable period for reconstruction. For the calculation of the SPEI indexes, we made use of the R code used in generating the SPEIbase (Beguería, 2022).

The spatial stability of the correlations between our reconstruction and the Standardized Precipitation Evapotranspiration Index (SPEI) was assessed using the SPEI for an accumulation period of 9 months (SPEI9). The relationship between our reconstruction and the large-scale atmospheric circulation was analyzed using the monthly means of geopotential height at 500 mb (Z500), zonal wind at 500 mb (U500), and meridional wind at 500 mb (V500) and at 200 mb (V200) from the Twentieth Century Reanalysis (V3) dataset ($2^\circ \times 2^\circ$ grid, 1837–2015 CE). Sea surface temperature (SST) data were extracted from the ERSST V5 dataset ($2^\circ \times 2^\circ$, 1854–2020). These datasets offer extended temporal coverage ($\sim$ 180 years for atmospheric, $\sim$ 167 years for oceanic) and have been successfully used in paleoclimate studies (Ionita et al., 2021; Nagavciuc et al., 2022a; Roibu et al., 2022).

2.4 Statistical methods and reconstruction model

The spatial stability of the $\delta^{18}O$–SPEI relationship was tested by using so-called stability maps, a methodology successfully used to examine the stationarity of the long-term relationship in seasonal river forecasts (Ionita et al., 2018, 2015, 2008) and dendrochronological studies (Nagavciuc et al., 2019a, 2022a; Roibu et al., 2022). In order to detect stable predictors, the variability of the correlation between the tree ring parameters and the gridded data is investigated within a 31-year moving window over the analyzed period. A correlation was considered to be stable in regions where tree ring parameters and gridded data exhibited significant correlations at the 90 % or 80 % levels for over 80 % of the sliding-window period. The basic idea of this approach is to pinpoint regions where the correlation between the tree ring parameters and the gridded data remains consistent over time.

For drought reconstruction, we used the August SPEI for the accumulation period of 9 months (Aug SPEI9) covering the period 1900–2020 over the eastern part of Europe. The reconstruction model was developed using the R packages dplR (Bunn, 2008) and treeclim (Zang and Biondi, 2015) using the linear regression model. The reconstructed model's predictive skills were tested by splitting the chronology into calibration and verification periods and calculating statistics, including the coefficient of determination (R^2), the reduction of error (RE), and the coefficient of efficiency (CE), where RE and CE values of > 0 were required (Briffa and Jones, 1992). Additionally, the Durbin–Watson statistic (DW) was used to test the trend in the residuals (Durbin and Watson, 1950). The model calibration was carried out for the 120-year period between 1900 and 2020. The two equal periods of calibration and verification statistics were both made up of two 60-year sub-periods from 1900 to 1960 and from 1961 to 2020.

The influence of the large-scale atmospheric circulation on the variability of $\delta^{18}O$ in the tree ring cellulose of Letea Forest was analyzed by computing composite maps for the years characterized by high $\delta^{18}O$ values (i.e., $\delta^{18}O > 1$ standard deviation) and low $\delta^{18}O$ values (i.e., $\delta^{18}O < -1$ standard deviation). The number of extreme years in the reconstructed August SPEI9 for the past 200 years was determined by counting the years that fall outside the range of values contained between the 10th percentile (0.1 quantile) and the 90th percentile (0.9 quantile).

The synchronicity of our reconstruction with other reconstructions was tested by analyzing the four previously published reconstructions available in the surrounding area: one August SPEI3 from eastern Carpathian, Romania (Nagavciuc et al., 2022a); one September SPEI6 from the Czech Republic (Brázdil et al., 2016); one precipitation reconstruction from the eastern Black Sea region, Turkey (Akkemik et al., 2005); and one streamflow reconstruction for the lower Danube River at Ceatal Izmail hydrometric station (Nagavciuc et al., 2023).

3 Results and discussion

3.1 Characteristics of oxygen isotope chronology

The $\delta^{18}O$ chronology was developed based on the seven individual measured $\delta^{18}O$ time series from Letea Forest, Romania (Fig. 1), and covers the 1803–2020 period. The $\delta^{18}O$

values of the combined chronology vary around the mean of 27.9 ‰, ranging from 26.1 ‰, recorded in 1941, to 29.7 ‰, recorded in 1863 (Fig. S1 in the Supplement). The first-order autocorrelation for $\delta^{18}O$ data (AC1) is 0.47, and this decreases to 0.21 for the second-order autocorrelation (AC2). The mean sample replication for the analyzed period is seven series; a smaller replication is only available between 1803 and 1813, where the replication reaches four series. Acting as a confirmation of literature results (Duffy et al., 2019), our $\delta^{18}O$ series show no juvenile effects or common increasing or decreasing trends in the first 140 years of tree age; therefore, we conclude that $\delta^{18}O$ values from oak tree ring cellulose from Letea Forest can be used for dendroclimatological studies without any detrending procedure.

3.2 Hydroclimate–$\delta^{18}O$ value relationships

Climate signal strength in the oxygen isotope chronology was evaluated by computing the monthly and seasonal (different combinations of months) Pearson's correlations between the $\delta^{18}O$ values and different climatic parameters available from the Sulina meteorological station for 52 years (1961–2013) (Fig. 2). Our results show significant ($p < 0.05$) and negative correlations with JJA cloud cover ($r = -0.54$), with J–A precipitation ($r = -0.39$), and with JJA relative humidity ($r = -0.49$), and they show significant and positive correlations with JJA sunshine duration ($r = 0.47$) and with J–A maximum temperature ($r = 0.44$), mean temperature ($r = 0.39$), and minimum temperature ($r = 0.28$).

The obtained correlations between our $\delta^{18}O$ chronology and monthly cloud cover, relative humidity, and precipitation are higher compared with the obtained correlations between our $\delta^{18}O$ chronology and monthly sunshine duration and temperature; these findings suggest that the variability in $\delta^{18}O$ in oak tree ring cellulose in the studied area is primarily influenced by moisture conditions, with higher $\delta^{18}O$ values being associated with drier conditions and with lower $\delta^{18}O$ values being associated with wetter conditions. Moisture conditions (high cloud cover, relative humidity, precipitation, and low temperatures) determine higher stomatal conductance and a lower transpiration rate, which leads to lower $\delta^{18}O$ values in tree ring cellulose. Conversely, dry climatic conditions (periods of reduced precipitation, low relative humidity, and higher temperatures) determine the reduction in stomatal conductance and the higher transpiration rate, which lead to higher $\delta^{18}O$ values in their cellulose (Siegwolf et al., 2022; McCarroll and Loader, 2004).

We have also tested the relationship between $\delta^{18}O$ values and the SPEI at Sulina station, with different accumulation periods (e.g., 1, 3, 6, 9, and 12 months). The obtained results reveal that the $\delta^{18}O$ values are significant (95 % significance level) and negatively correlated with all tested SPEI drought indices from the summer months. Correlation coefficients were found to be lower for shorter timescales (e.g., SPEI1, SPEI3), but they increased for longer timescales (SPEI 6, SPEI9) (Figs. 3, S2). The Letea $\delta^{18}O$ chronology is significantly and negatively correlated with July SPEI1 ($r = -0.42$, $p < 0.05$), with August SPEI3 ($r = -0.57$, $p < 0.05$), with August SPEI6 ($r = -0.60$, $p < 0.05$), and with Aug SPEI12 ($r = -0.57$, $p < 0.05$), and the highest correlation coefficient was obtained for August SPEI9 ($r = -0.63$, $p < 0.05$). The obtained significant correlations imply that the $\delta^{18}O$ values in the oak tree ring cellulose from Letea Forest are constrained by water availability. The higher correlation with the drought index compared to temperature or precipitation suggests that the SPEI is a more effective indicator of moisture levels than using precipitation or temperature alone as it considers both precipitation and temperature through evapotranspiration demand. The obtained higher correlation for longer timescales (e.g., SPEI9) compared to that for shorter timescales (e.g., SPEI1) indicates that the $\delta^{18}O$ values in this area tend to respond more significantly to drought over extended periods (Gessler et al., 2014; Roden et al., 2000).

The spatio-temporal stability of hydroclimatic signals was tested by applying the stability map approach between the $\delta^{18}O$ values and the gridded mean temperature (TT), precipitation (PP), and SPEI9 data over the period 1901–2020 based on the CRU TS v. 4.04 data (Harris et al., 2020). Stability map analyses with precipitation show a significant and stable correlation in summer over the eastern part of Romania, the Republic of Moldova, and the central part of Ukraine (Fig. S3). The results obtained for stability maps with temperature show a significant and stable correlation in April over central and northern Europe, in June over southwestern Europe, in August over Hungary and Slovakia, in March–April–May over central Europe, and in June–July–August over the southern part of France (Fig. S4).

Stability maps for $\delta^{18}O$ values and SPEI9 data reveal a significant and stable correlation starting in February and extending until October, including spring (March–April–May) and summer (June–July–August) (Fig. 4). In February and March, the correlation is significant and stable over a small region in the southeastern part of Romania and the southern part of the Republic of Moldova, the region where our study site is located. Starting in April, the area exhibiting a stable and significant correlation begins to expand, encompassing Romania, the Republic of Moldova, the central part of Ukraine, and the eastern part of Bulgaria. From June onwards, the stable correlation extends to the eastern part of Europe and continues to increase, reaching its peak in August. During this month, the largest area is covered by a stable and significant correlation, including the eastern and central parts of Europe (Fig. 4). According to monthly correlation analyses and the stability map approach, we identified the August SPEI9 over the central and eastern parts of Europe (see the black square in Fig. 4) as the most appropriate predictor for drought reconstruction.

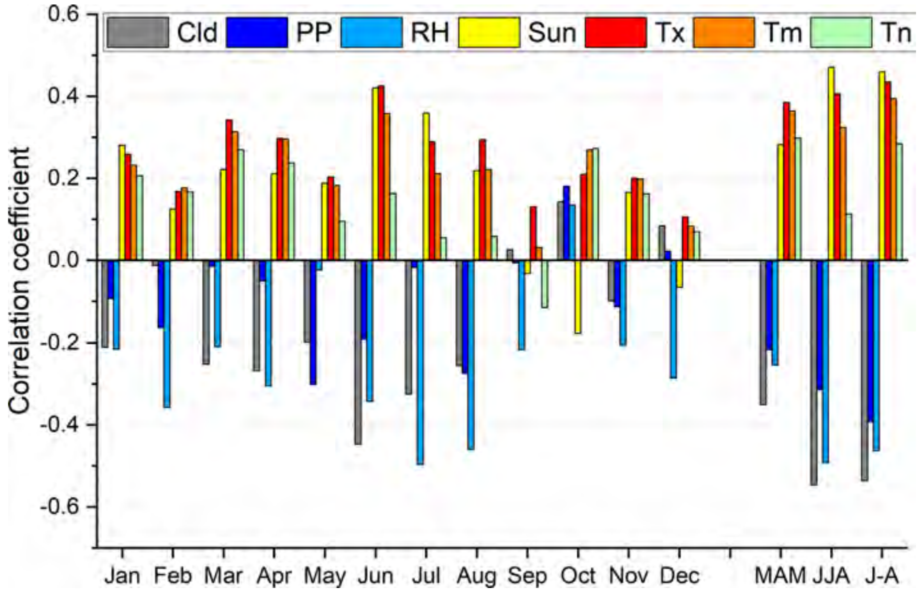

Figure 2. The correlation coefficients of $\delta^{18}O$ chronology from Letea Forest with monthly climate data (cloud cover – Cld, precipitation – PP, relative humidity – RH, sunshine duration – sun, maximum temperature – Tx, mean temperature – Tm, minimum temperature – Tn) from Sulina meteorological station. Correlation analyses were performed from January to December but also for March, April, and May (MAM); June, July, and August (JJA); and January to August (J–A). The dotted black lines represent the significance level at 0.05.

Table 1. Calibration and verification statistics for the August SPEI9 reconstruction based on $\delta^{18}O$ values from Letea Forest. Analyzed period: 1901–2020. Statistics include the correlation coefficient (r), the coefficient of determination (r^2), the reduction of error (RE), the coefficient of efficiency (CE), and the Durbin–Watson statistic (DW).

Subset lengths	r	r^2	RE	CE	DW
Early calibration (1901–1960) and late verification (1961–2020)	−0.67	0.45	0.34	0.34	1.96
Early verification (1901–1960) and late calibration (1961–2020)	−0.62	0.38	0.35	0.35	1.64
Full calibration period (1922–2013)	−0.63	0.40			

Figure 3. Correlation analyses between $\delta^{18}O$ values and SPEI drought index with different time windows: SPEI1, SPEI3, SPEI6, SPEI9, and SPEI12 from January to September (95 % significance level).

3.3 Drought reconstruction

In order to reconstruct the drought variability for the last 200 years, we used the August SPEI9 over the central and eastern parts of Europe (see the black square in Fig. 4) as the predictand and the $\delta^{18}O$ chronology from Letea Forest as the predictor. The reconstruction was developed using the linear regression model. Reconstruction skills were evaluated by splitting our chronology into two equally long periods (1901–1960 and 1961–2020) for the calibration–verification approach in forward and reverse mode (Fig. 5). The calibration and verification models passed all the conventional verification tests in both the forward and reverse modes. The positive values obtained for the reduction of error (RE) and coefficient of efficiency (CE) in the forward and reverse modes (Table 1) indicate good and predictive reconstruction skills. These results are supported by a DW value near 2, which indicates low to no autocorrelation. Therefore, the obtained statistical results suggest that the linear regression model used is reliable, with high predictive skill for the August SPEI9

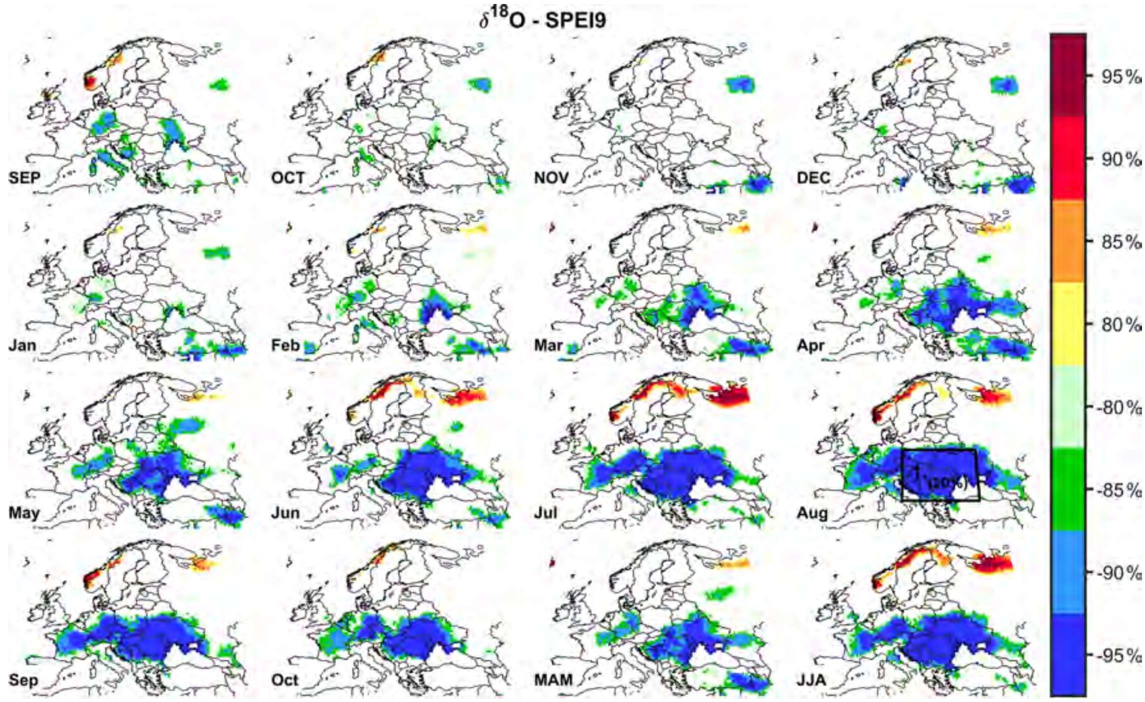

Figure 4. Stability map of the correlation between the δ^{18}O chorology and different monthly combinations of SPEI9 from September in the previous year until October in the current year but also for the March, April, and May (MAM) and June, July, and August (JJA) periods. Regions where the correlation is stable, positive, and significant for at least 80 % of windows are shaded with dark red (95 %), red (90 %), orange (85 %), and yellow (80 %). The corresponding regions where the correlation is stable but negative are shaded with dark blue (95 %), blue (90 %), green (85 %), and light green (80 %). Analyzed period: 1902–2020. The significance level is computed based on a two-tailed t test.

reconstruction over the central and eastern parts of Europe. The developed reconstruction model can be used to reconstruct past long-term drought variability; it explains 40 % ($r^2 = 0.40$) of the drought variation over the analyzed region.

The interannual to interdecadal variations in our August SPEI9 drought reconstruction for the period 1807–2020 are presented in Fig. 6. The tree ring reconstruction generally matches both the interannual and decadal variability in the observed August SPEI9 variability (Fig. 5). According to our results, the wettest long-term periods occurred between 1905–1915, 1934–1944, 1951–1958, and 1980–1995. The driest periods occurred between 1818–1835, 1845–1854, 1882–1890, and 2007–2020, maintaining the decreasing trend. Interestingly, the dry and wet periods are not evenly distributed across time. The most wet periods were recorded during the 20th century, while the long-term dry periods were recorded in the 19th and 21st centuries. Also, a clear trend of increasing drought conditions has been observed for the analyzed region since the year 2000, in agreement with recent studies (Info Clima, 2024; Nagavciuc et al., 2022b).

The extremes in the August SPEI9 reconstruction over the last 200 years were summarized by counting the number of years outside the 0.1 and 0.9 quantiles. Over the analyzed period, we identified 31 extremely positive (wet) years and 31 extremely negative (dry) years. The most extreme positive years are 1954 and 1809 (1.82), 1906 (1.93), 1907 (2.07), 1908 (2.37), and 1941 (2.74), and the most extreme negative years are 1873 (−2.10), 1834 (−2.16), 1833 (−2.20), 1822 (−2.20), and 1863 (−2.86). The occurrence frequency of the extreme years corresponds with the distribution of the decadal variability. Only 5 extreme wet years were recorded in the 19th century, and only 4 extreme dry years were recorded in the 20th century. The longest interval with continuous dry events is 10 years, occurring between 2011 and 2020. Similarly, the maximum interval with continuous wet events was also 10 years, occurring between 1906 and 1915.

3.4 δ^{18}O variability and large-scale atmospheric circulation

Previous studies have shown that the low- and high-frequency variabilities of δ^{18}O values in tree ring cellulose over Europe are also influenced by the prevailing large-scale atmospheric circulation and the sea surface temperature (SST) (Ionita, 2015; Roibu et al., 2022; Nagavciuc et al., 2019b). According to our results, years with a high δ^{18}O value are associated with a high-pressure system over the North Atlantic Ocean, extending towards the central and

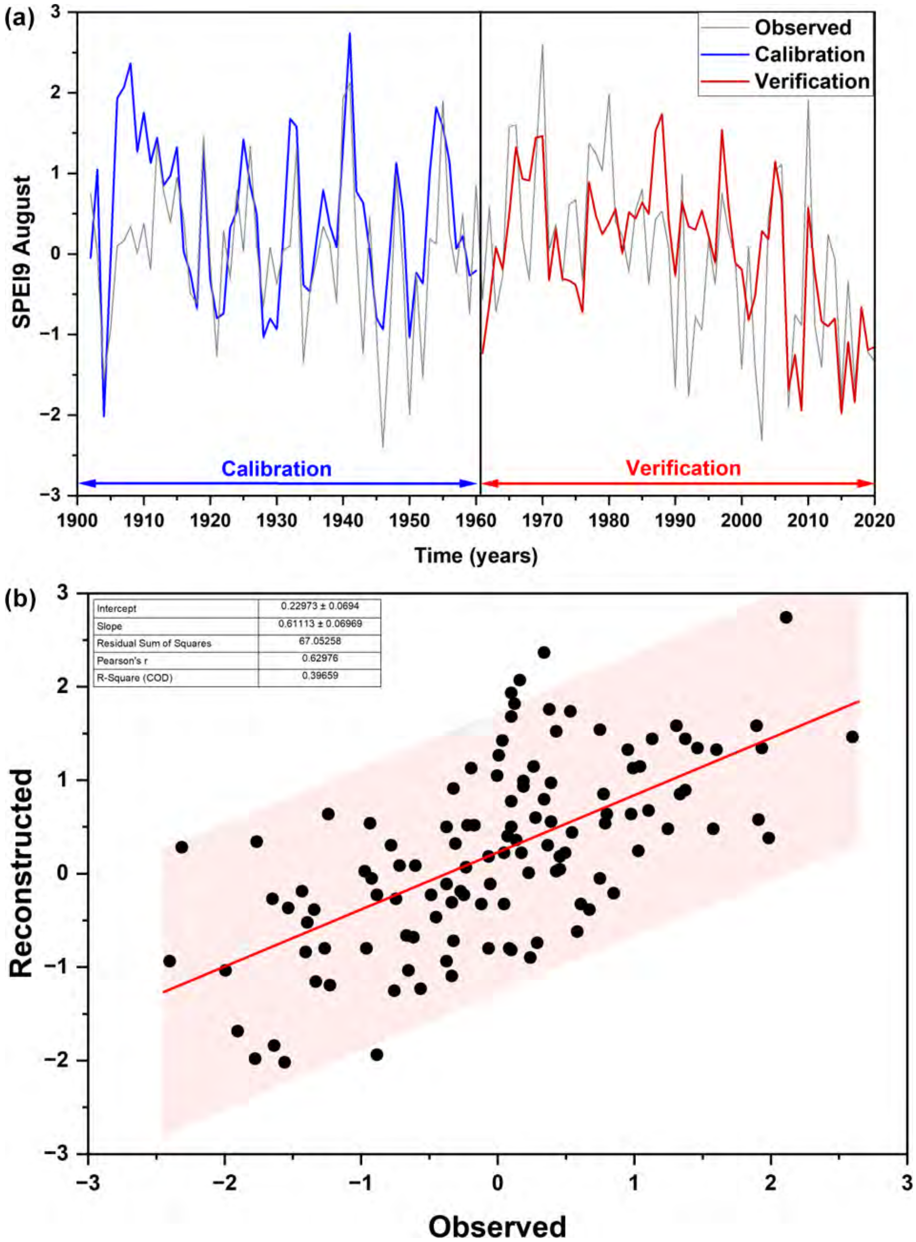

Figure 5. **(a)** Calibration–verification model for the August SPEI9 reconstruction; the gray line indicates the observed data (CRU TS v. 4.04 dataset, Harris et al., 2020), the red line indicates the reconstructed August SPEI9 over the calibration period, and the blue line indicates the reconstructed August SPEI9 over the verification period. **(b)** Regression between the observed and reconstructed August SPEI9 over the period 1900–2020.

eastern parts of Europe, and a center of low-pressure anomalies south of Greenland (Fig. 7).

This type of large-scale structure over the central and southern parts of Europe suppresses ascending motions and reduces water vapor condensation and precipitation formation. Consequently, this leads to drought conditions in the land surface areas beneath this system, including our study region (Fig. 7a). This pattern is linked to Rossby wave oscillation, as captured by the meridional wind at 200 mb, and is associated with high $\delta^{18}O$ values (Fig. 7c). Shifts in the direction and intensity of meridional winds can contribute to the formation and persistence of blocking high-pressure systems. These systems act as barriers to the typical transport of moisture-laden air masses from the Atlantic or Mediterranean, hindering precipitation over eastern Europe. In contrast, low values of $\delta^{18}O$ are associated with negative Z500 anomalies extending from the central Atlantic to Europe (Fig. 7b). The center of negative Z500 anomalies over Eu-

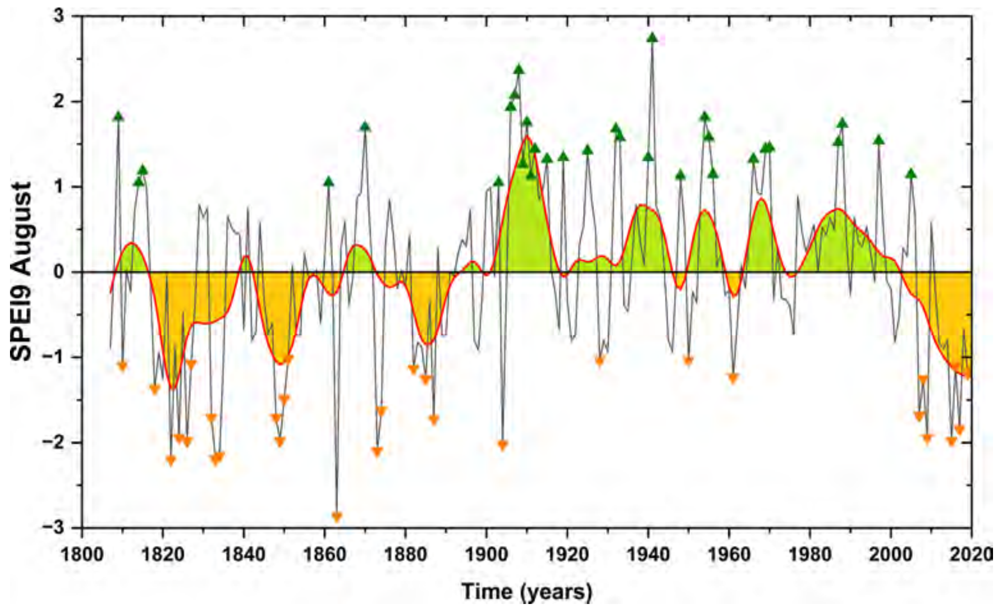

Figure 6. Reconstructed August SPEI9 (black line) for the 1807–2020 period, with a 31-year running mean (red line). Extreme dry and wet years are represented by lower-orange and upper-green triangles, respectively. Extreme years are defined as those in which the August SPEI9 index falls below −1.5 or exceeds +1.5 standard deviations.

rope is consistent with enhanced precipitation in our study region due to the advection of moisture from the Mediterranean and Black seas (Fig. 7b). Low δ^{18}O values are also associated with the prevalence of a hemispheric-wave-4 pattern (Fig. 7d), a pattern found to be linked with drought and heatwaves, depending on the location of its centers of action (Yang et al., 2024).

Similar large-scale structures have been found to be associated with δ^{18}O extreme values in the Călimani Mountains (Nagavciuc et al., 2020, 2022a). The δ^{18}O variability, both at the European level and more regionally, has been found to be influenced by the sea surface temperature anomalies, especially in the North Atlantic basin (Nagavciuc et al., 2024a). In the current case, high values of δ^{18}O in tree ring cellulose are associated with positive SST anomalies in the North Atlantic Ocean, the Mediterranean region, and the Black Sea and with negative SST anomalies in the central Atlantic Ocean (Fig. 7e). In contrast, low δ^{18}O values correspond to negative SST anomalies over the Mediterranean Sea and the Black Sea and to positive SST anomalies over the central Atlantic Ocean (Fig. 7f). This particular SST pattern has been found to strongly affect the dry and wet conditions in the central and eastern parts of Europe, especially on decadal and multidecadal timescales, by influencing the prevailing large-scale atmospheric circulation (Ionita et al., 2022). Overall, in this section, we show that the combined impact of atmospheric and oceanic circulation is reflected in the δ^{18}O of tree rings from the eastern part of Europe. Disentangling the complex interplay of factors affecting the variability of δ^{18}O in tree ring cellulose is crucial for accurate climate reconstructions. Studies often integrate tree ring data with climate models and other paleoclimate proxy data to gain a holistic understanding of past climate variations driven by shifts in atmospheric and oceanic circulation patterns.

3.5 Comparison with other records

Other dendroclimatic studies from eastern Europe indicate a moisture sensitivity of the tree ring parameters. To test the synchronicity of our reconstruction, we compared the obtained August SPEI9 reconstruction with four previously published reconstructions available in the surrounding area. We have selected two drought reconstructions: one August SPEI3 from the eastern Carpathians, Romania (Nagavciuc et al., 2022a), and one September SPEI6 from the Czech Republic (Brázdil et al., 2016). Additionally, we included precipitation reconstruction from the eastern Black Sea region, Turkey (Akkemik et al., 2005), and a streamflow reconstruction for the lower Danube River at Ceatal Izmail hydrometric station (Nagavciuc et al., 2023) (Fig. 8). The results showed good synchronicity between analyzed reconstructions, maintaining both high- and low-frequency variability, similarly to other reconstructions. The analyzed reconstructions present similar features of low frequency, with clear common characteristics that are coherent over a large spatial scale. For example, the low frequency of the reconstructed August SPEI9 in this study agrees with the summer drought August SPEI3 (Nagavciuc et al., 2022a) and the lower Danube streamflow (Nagavciuc et al., 2023). The observed low-frequency differences among the analyzed reconstructions may be attributed to their varying temporal scales. Our study employed

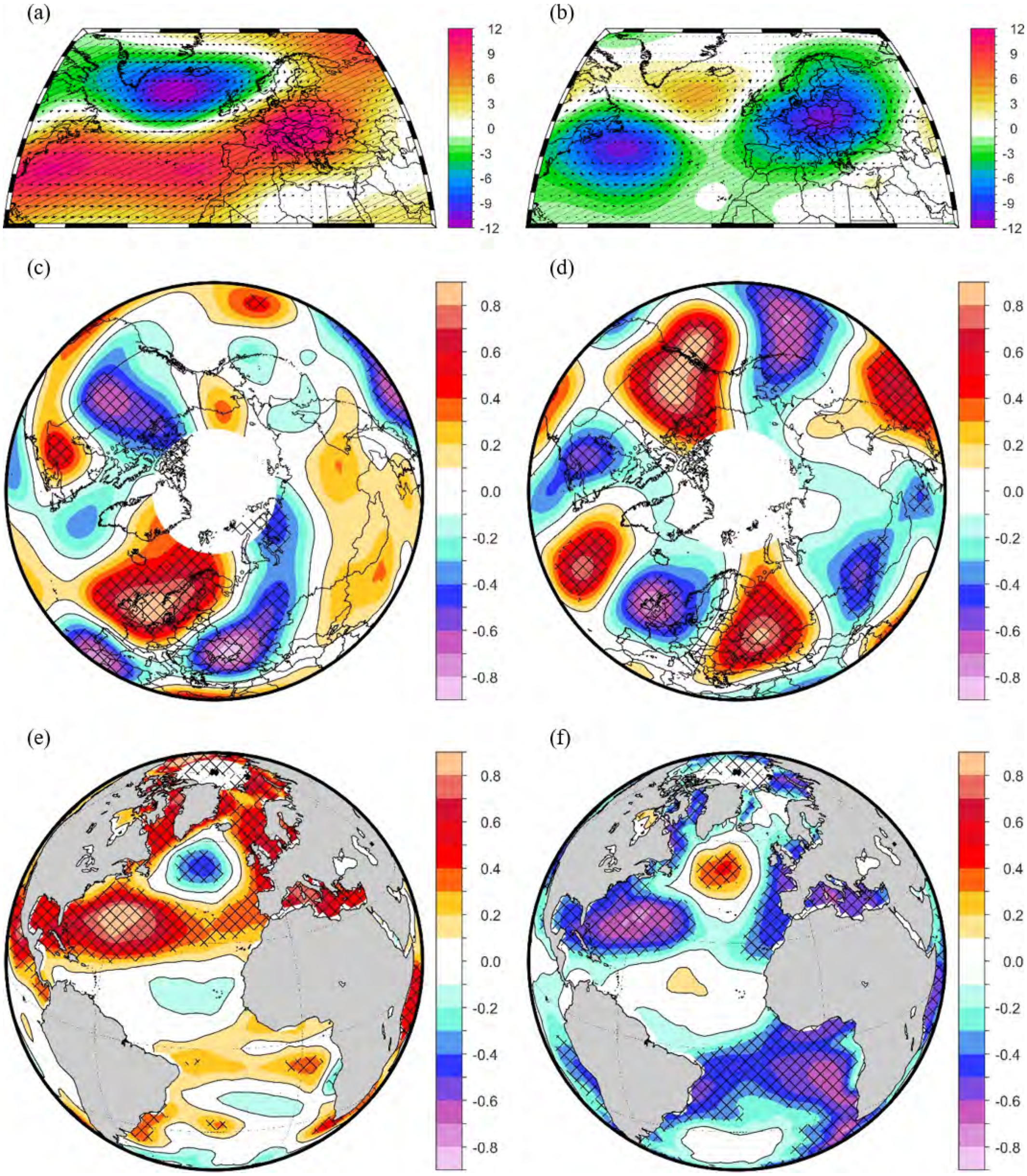

Figure 7. **(a)** The composite map between high δ^{18}O values (> 1 SD) and the annual (mean over the period of December in the previous year until August in the current year) geopotential height at 500 mb (Z500), **(b)** the same as **(a)** but for low δ^{18}O values (< −1 SD), **(c)** as in **(a)** but for the meridional wind at 200 mb (V200), **(d)** as in **(b)** but for the meridional wind at 200 mb (V200), **(e)** as in **(a)** but for the sea surface temperature, and **(f)** as in **(b)** but for the sea surface temperature. The hatching highlights significant correlation coefficients at a confidence level of 95 %. Units: Z500 (m). Analyzed period: 1836–2020 for Z500 and V200 and 1855–2020 for the SST.

a longer time frame (SPEI9), while the others utilized shorter periods (SPEI6 or SPEI3).

A more detailed investigation of the selected reconstructions reveals a good agreement in terms of high-frequency variability, with significant correlations. The highest coefficient of correlation was obtained with the August SPEI3 reconstruction from the Calimani Mountains, Romania ($r = 0.38$), likewise based on δ^{18}O in tree ring cellulose. This is followed by the lower Danube streamflow reconstruction based on tree ring width from Caraorman Forest, Danube Delta, Romania ($r = 0.37$). Lower but significant correlations were found with the September SPEI6 drought reconstruction in the Czech Republic ($r = 0.28$) based on historical documents and with the May–June precipitation record from the eastern Black Sea region, Turkey ($r = 0.21$), derived from tree ring width analysis.

Another important aspect regarding the similarities between analyzed reconstruction is the occurrence of the ex-

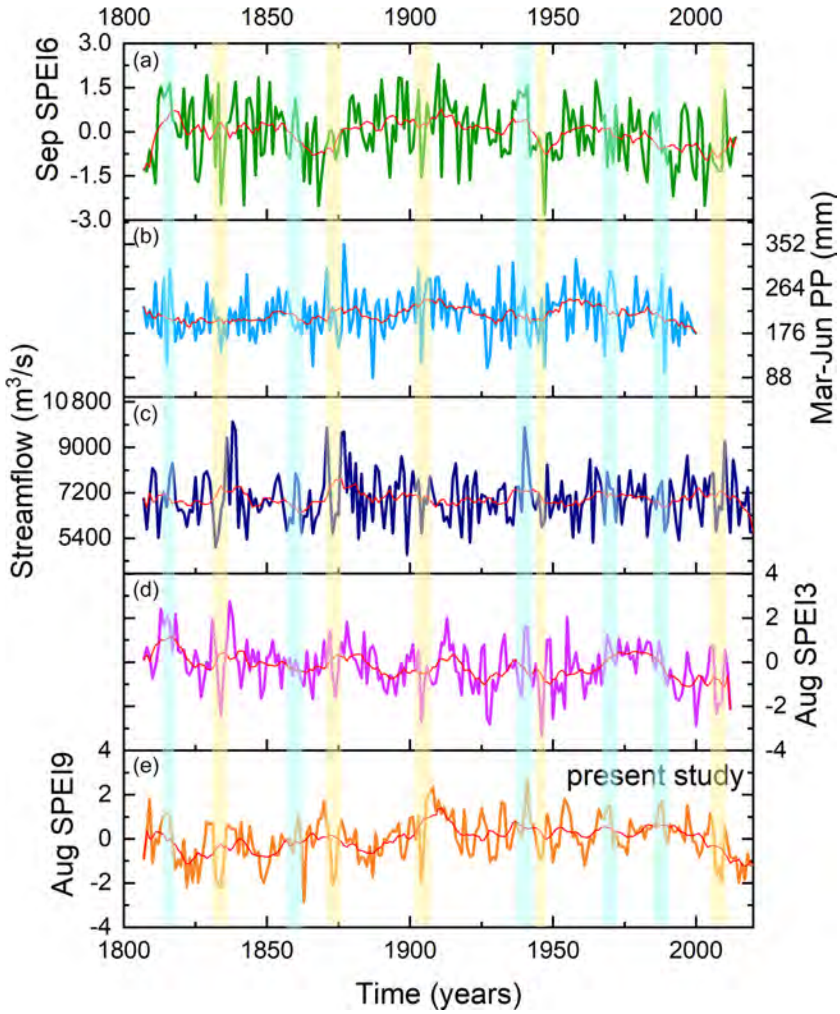

Figure 8. Comparison between different reconstructions of **(a)** September SPEI6 from the Czech Republic (Brázdil et al., 2016); **(b)** precipitation reconstructions from the eastern Black Sea region, Turkey (Akkemik et al., 2005); **(c)** streamflow reconstructions for the lower Danube River at Ceatal Izmail hydrometric station (Nagavciuc et al., 2023); **(d)** August SPEI3 from eastern Carpathian, Romania (Nagavciuc et al., 2022a); and **(e)** August SPEI9 reconstructions (this study).

treme events. We have identified a large number of extreme climate events in all five reconstructions, both positive (e.g., 1814, 1861, 1941, 1969, 1988) and negative (e.g., 1834, 1873, 1904, 1946, 1950, 2007, 2008, 2009). The occurrence of these extreme events is documented in numerous historical records. For example, in 1834, a severe drought was recorded in the Moldova and Ardeal regions (Teodoreanu, 2017; Topor, 1963; Pfister, 1999; Nagavciuc et al., 2022a), as well as in the Czech lands (Brázdil et al., 2019, 2016). Additionally, a devastating drought occurred in central Turkey (Akkemik et al., 2008, 2005) during the same year. The year 1904 stands out in the records as the year of a devastating drought event in Moldova and Romania (Teodoreanu, 2017; Topor, 1963; Pfister, 1999; Nagavciuc et al., 2022a), as well as in the Czech lands (Brázdil et al., 2019, 2016). Furthermore, the years 1946, 2007, 2008, and 2009 are well known in the literature as extreme dry years. The wet events of our reconstruction are, likewise, mentioned in the documentary data. For example, 1814 was recorded as an extremely wet summer (Cernovodeanu and Binder, 1933; Pfister, 1999), not only in Romania but also in Turkey (Akkemik et al., 2005, 2008). As another example, 1941 has been recognized as the year of a very cold and rainy summer, with heavy rains (Teodoreanu, 2017; Topor, 1963; Nagavciuc et al., 2022a).

Our reconstruction aligns closely with existing studies on droughts and pluvials, revealing consistent patterns across different regions and time periods. Despite variations in methodologies, proxies, and seasonal focuses, there is a substantial consensus among the reconstructions, suggesting a stable relationship between climate variability and proxy data. This robust understanding provides a strong foundation for future climate projections and risk assessments. Although some discrepancies may arise due to differences in site locations or temporal resolutions, the overall agreement reinforces the reliability of the reconstructed climate trends and enhances our knowledge of past climate variability in the region. Moreover, the alignment between our reconstruction and others indicates that the climatic drivers responsible for past droughts and pluvial changes were likely to be widespread and persistent rather than localized or transient. This insight is essential for assessing the potential impacts of future climate change on regional water resources and ecosystems.

4 Conclusions

This study investigated the potential of δ^{18}O in oak tree ring cellulose from Letea Forest, Romania, as a proxy for reconstructing past drought variability. We developed a robust δ^{18}O chronology from the isotope time series of individual trees for the period 1807–2020 CE. We found a significant negative correlation between δ^{18}O and various climatic parameters, including precipitation, relative humidity, and cloud cover. Conversely, δ^{18}O showed a positive correlation with temperature and sunshine duration. These relationships suggest that δ^{18}O primarily reflects moisture availability in the study area. Nevertheless, the strongest correlation was found between δ^{18}O and the Standardized Precipitation Evapotranspiration Index (SPEI9) for August over central and eastern Europe. This highlights the superior sensitivity of δ^{18}O to hydroclimatic conditions (August SPEI9), particularly on longer timescales, compared to relationships with temperature or precipitation data alone. The good regional relationship between August SPEI9 and δ^{18}O was confirmed by stability maps.

Using a linear regression model, we developed a reconstruction of August SPEI9 for the past 200 years based on the δ^{18}O chronology. The August SPEI9 drought reconstruction reveals valuable information on the interannual and decadal climate variabilities of the central and eastern parts of Europe. According to our reconstruction, the wettest periods occurred during 1905–1915, 1934–1944, 1951–1958, and 1980–1995, and the driest periods occurred during 1818–1835, 1845–1854, 1882–1890, and 2007–2020. Interestingly, the most extreme wet periods occurred in the 20th century, while the most extreme dry periods were recorded in the 19th and 21st centuries.

Further analysis revealed that δ^{18}O variability is influenced by large-scale atmospheric circulation patterns. Years with high δ^{18}O values were associated with a high-pressure system over the North Atlantic, linked to Rossby wave oscillations and positive sea surface temperature anomalies. Conversely, years with low δ^{18}O values corresponded to negative pressure anomalies over Europe, indicating enhanced precipitation. Additionally, sea surface temperature anomalies in the North Atlantic, as well as in the Mediterranean and Black seas, correspond to high and low δ^{18}O values, suggesting an interplay between atmospheric and oceanic circulation in influencing moisture availability over the analyzed region.

Comparison with other paleoclimate reconstructions from the region (drought, precipitation, and streamflow reconstructions) revealed good synchronicity and agreement in terms of both low- and high-frequency variability, thus highlighting the robustness of our August SPEI9 reconstruction for central and eastern Europe.

Overall, this study demonstrates the valuable application of δ^{18}O in oak tree ring cellulose for reconstructing past hydroclimatic variability in Letea Forest of the Danube River delta and in central and eastern Europe. Combining tree ring δ^{18}O records with other paleoclimate proxies and climate models can provide a more comprehensive understanding of long-term climate dynamics and their drivers. Future research can further refine drought reconstructions by incorporating additional environmental data and expanding the spatial coverage by studying additional tree sites.

Data availability. The reconstructed August SPEI9 chronology for the 1807–2020 period is available here: https://doi.org/10.5281/zenodo.14536886 (Nagavciuc et al., 2024b).

Supplement. The supplement related to this article is available online at: https://doi.org/10.5194/bg-22-55-2025-supplement.

Author contributions. VN and MI designed the study and wrote the article draft. GH, MR, CCR, and MGC helped with writing the original draft and interpreting the results, as well as with the review process.

Competing interests. The contact author has declared that none of the authors has any competing interests.

Disclaimer. Publisher's note: Copernicus Publications remains neutral with regard to jurisdictional claims made in the text, published maps, institutional affiliations, or any other geographical representation in this paper. While Copernicus Publications makes every effort to include appropriate place names, the final responsibility lies with the authors.

Special issue statement. This article is part of the special issue "Drought, society, and ecosystems (NHESS/BG/GC/HESS inter-journal SI)". It is not associated with a conference.

Financial support. Viorica Nagavciuc and Monica Ionita were partially supported by a grant from the Ministry of Research, Innovation and Digitization under the "Romania's National Recovery and Resilience Plan – Founded by EU-NextGenerationEU" program, project "Compound extreme events from a long-term perspective and their impact on forest growth dynamics (CExForD)" (project no. 760074/23.05.2023, code 287/30.11.2022, within Pillar III, Component C9, Investment 8). Monica Ionita was also supported by the Helmholtz Association through the joint program "Changing Earth – Sustaining our Future" (PoF IV) of the AWI and the Helmholtz Climate Initiative REKLIM.

The article processing charges for this open-access publication were covered by the Alfred Wegener Institute Helmholtz Centre for Polar and Marine Research.

Review statement. This paper was edited by Mana Gharun and reviewed by Marzena Kłusek and one anonymous referee.

References

Abdelazim, M. N. and Diaconu, D. C. (Eds.): The Danube River Delta, Earth and., Springer, Cham, Switzerland, 402 pp., https://doi.org/10.1007/978-3-031-03983-6, 2022.

Akkemik, Ü., Dağdeviren, N., and Aras, A.: A Preliminary Reconstruction (A.D. 1635–2000) of Spring Precipitation Using Oak Tree Rings in the Western Black Sea Region of Turkey, Int. J. Biometeorol., 49, 297–302, https://doi.org/10.1007/s00484-004-0249-8, 2005.

Akkemik, Ü., D'arrigo, R., Cherubini, P., Kose, N., and Jacoby, G. C.: Tree-ring reconstructions of precipitation and streamflow for north-western, Int. J. Climatol., 28, 173–183, 2008.

Allen, S. T., Kirchner, J. W., Braun, S., Siegwolf, R. T. W., and Goldsmith, G. R.: Seasonal origins of soil water used by trees, Hydrol. Earth Syst. Sci., 23, 1199–1210, https://doi.org/10.5194/hess-23-1199-2019, 2019.

Baker, J. C. A., Cintra, B. B. L., Gloor, M., Boom, A., Neill, D., Clerici, S., Leng, M. J., Helle, G., and Brienen, R. J. W.: The Changing Amazon Hydrological Cycle Inferences From Over 200 Years of Tree-Ring Oxygen isotope data, J. Geophys. Res.-Biogeo., 127, e2022JG006955, https://doi.org/10.1029/2022JG006955, 2022.

Beguería, S.: sbegueria/SPEIbase: Version 2.7, Zenodo, https://doi.org/10.5281/zenodo.5864391, 2022.

Brázdil, R., Dobrovolný, P., Trnka, M., Büntgen, U., Řezníčková, L., Kotyza, O., Valášek, H., and Štěpánek, P.: Documentary and instrumental-based drought indices for the Czech Lands back to AD 1501, Clim. Res., 70, 103–117, https://doi.org/10.3354/cr01380, 2016.

Brázdil, R., Dobrovolný, P., Trnka, M., Řezníčková, L., Dolák, L., and Kotyza, O.: Extreme droughts and human responses to them: the Czech Lands in the pre-instrumental period, Clim. Past, 15, 1–24, https://doi.org/10.5194/cp-15-1-2019, 2019.

Briffa, K. and Jones, P.: Basic chronology statistics and assessment, in: Methods of dendrochronology, edited by: Cook, E. and Kairiukstis, L., Kluwer, Dordrecht, 137–152, 1992.

Bunn, A. G.: A dendrochronology program library in R (dplR), Dendrochronologia, 26, 115–124, https://doi.org/10.1016/j.dendro.2008.01.002, 2008.

Cernovodeanu, P. and Binder, P.: Cavalerii Apocalipsilui Calamită?ile naturale din trecutul României (până la 1800), SILEX-Casă de Editură, Presă ?i Impresarial S.R.L., Bucuresti, ISBN 973-95477-3-7, 1933.

Coplen, T. B.: Reporting of stable hydrogen, carbon, and oxygen isotopic abundances, Pure Appl. Chem., 66, 273–276, https://doi.org/10.1351/pac199466020273, 1994.

CDendro and CooRecorder: Software tools: CDendro and CooRecorder, http://www.cybis.se/forfun/dendro/index.htm (last access: 20 February 2024), 2010.

Dansgaard, W.: Stable isotopes in precipitation, Tellus, 4, 436–468, https://doi.org/10.3402/tellusa.v16i4.8993, 1964.

Duffy, J. E., McCarroll, D., Loader, N. J., Young, G. H. F., Davies, D., Miles, D., and Bronk Ramsey, C.: Absence of Age-Related Trends in Stable Oxygen Isotope Ratios From Oak Tree Rings, Global Biogeochem. Cy., 33, 841–848, https://doi.org/10.1029/2019GB006195, 2019.

Durbin, J. and Watson, G. S.: Testing for Serial Correlation in Least Squares Regression: I, Biometrika, 37, 409–428, https://doi.org/10.2307/2332391, 1950.

Feng, X., Huang, R., Zhu, H., Liang, E., Bräuning, A., Zhong, L., Gong, Z., Zhang, P., Asad, F., Zhu, X., and Grießinger, J.: Tree-ring cellulose oxygen isotopes indicate atmospheric aridity in the western Kunlun Mountains, Ecol. Indic., 137, 108776, https://doi.org/10.1016/j.ecolind.2022.108776, 2022.

Freund, M. B., Helle, G., Balting, D. F., Ballis, N., Schleser, G. H., and Cubasch, U.: European tree-ring isotopes indicate unusual recent hydroclimate, Commun. Earth Environ., 4, 26, https://doi.org/10.1038/s43247-022-00648-7, 2023.

Gagen, M., Battipaglia, G., Daux, V., Duffy, J., Dorado-Liñán, I., Hayles, L. A., Martínez-Sancho, E., McCarroll, D., Shestakova, T. A., and Treydte, K.: Climate Signals in Stable Isotope Tree-Ring Records, vol 8, Springer, Cham., https://doi.org/10.1007/978-3-030-92698-4_19, 2022.

Gärtner, H. and Nievergelt, D.: The core-microtome: A new tool for surface preparation on cores and time series analysis of varying cell parameters, Dendrochronologia, 28, 85–92, https://doi.org/10.1016/j.dendro.2009.09.002, 2010.

Gessler, A., Ferrio, J. P., Hommel, R., Treydte, K., Werner, R. A., and Monson, R. K.: Stable isotopes in tree rings: Towards a mechanistic understanding of isotope fractionation and mixing processes from the leaves to the wood, Tree Physiol., 34, 796–818, https://doi.org/10.1093/treephys/tpu040, 2014.

Gessler, A., Bächli, L., Rouholahnejad Freund, E., Treydte, K., Schaub, M., Haeni, M., Weiler, M., Seeger, S., Marshall, J., Hug, C., Zweifel, R., Hagedorn, F., Rigling, A., Saurer, M., and Meusburger, K.: Drought reduces water uptake in beech from the drying topsoil, but no compensatory uptake occurs from deeper soil layers, New Phytol., 233, 194–206, https://doi.org/10.1111/nph.17767, 2022.

Harris, I., Osborn, T. J., Jones, P., and Lister, D.: Version 4 of the CRU TS monthly high-resolution gridded multivariate climate dataset, Sci. Data, 7, 1–18, https://doi.org/10.1038/s41597-020-0453-3, 2020.

Helle, G., Pauly, M., Heinrich, I., Schollän, K., Balanzategui, D., and Schürheck, L.: Stable Isotope Signatures of Wood, its Constituents and Methods of Cellulose Extraction, in: Stable Isotopes in Tree Rings: Inferring Physiological, Climatic and Environmental Responses, edited by: Siegwolf, R. T. W., Brooks, J. R., Roden, J., and Saurer, M., Springer International Publishing, Cham, 135–190, https://doi.org/10.1007/978-3-030-92698-4_5, 2022.

Holmes, R. L.: Computer-assisted quality control in tree-ring dating and measurement, Tree Ring Bull., 43, 69–75, 1983.

Info Clima: Starea Climei Romania, Bucharest, 1–101, https://static1.squarespace.com/static/60b5d21e4796a564a563c771/t/6722504d024790327172d799/1730302041386/Starea_Climei-Raport_2024.pdf (last access: 20 Norvember 2024), 2024.

Ionita, M.: Interannual summer streamflow variability over Romania and its connection to large-scale atmospheric circulation, Int. J. Climatol., 35, 4186–4196, https://doi.org/10.1002/joc.4278, 2015.

Ionita, M. and Nagavciuc, V.: Changes in drought features at the European level over the last 120 years, Nat. Hazards Earth Syst. Sci., 21, 1685–1701, https://doi.org/10.5194/nhess-21-1685-2021, 2021.

Ionita, M., Lohmann, G., and Rimbu, N.: Prediction of spring Elbe discharge Based on stable teleconnections with winter global temperature and precipitation, J. Climate, 21, 6215–6226, https://doi.org/10.1175/2008JCLI2248.1, 2008.

Ionita, M., Dima, M., Lohmann, G., Scholz, P., and Rimbu, N.: Predicting the June 2013 European Flooding Based on Precipitation, Soil Moisture, and Sea Level Pressure, J. Hydrometeorol., 16, 598–614, https://doi.org/10.1175/JHM-D-14-0156.1, 2015.

Ionita, M., Scholz, P., Grosfeld, K., and Treffeisen, R.: Moisture transport and Antarctic sea ice: austral spring 2016 event, Earth Syst. Dynam., 9, 939–954, https://doi.org/10.5194/esd-9-939-2018, 2018.

Ionita, M., Caldarescu, D. E., and Nagavciuc, V.: Compound Hot and Dry Events in Europe: Variability and Large-Scale Drivers, Front. Clim., 3, 688991, https://doi.org/10.3389/fclim.2021.688991, 2021.

Ionita, M., Nagavciuc, V., Scholz, P., and Dima, M.: Long-term drought intensification over Europe driven by the weakening trend of the Atlantic Meridional Overturning Circulation, J. Hydrol. Reg. Stud., 42, 101176, https://doi.org/10.1016/j.ejrh.2022.101176, 2022.

IPCC: Summary for policymakers, in: Climate Change 2021: The Physical Science Basis. Contribution of Working Group I to the Sixth Assessment Report of the Intergovernmental Panel on Climate Change, edited by: Masson-Delmotte, V., Zhai, P., Pirani, A., Connors, S. L., Péan, C., Berger, S., Caud, N., Chen, Y., Goldfarb, L., Gomis, M. I., Huang, M., Leitzell, K., Lonnoy, E., Matthews, J. B. R., Maycock, T. K., Waterfield, T., Yelekçi, O., Yu, R., and Zhou, B., Cambridge University Press, Cambridge, United Kingdom and New York, NY, USA, 3–22, https://doi.org/10.1017/9781009157896.001, 2021.

Kreibich, H., Van Loon, A. F., Schröter, K., Ward, P. J., Mazzoleni, M., Sairam, N., Abeshu, G. W., Agafonova, S., AghaKouchak, A., Aksoy, H., Alvarez-Garreton, C., Aznar, B., Balkhi, L., Barendrecht, M. H., Biancamaria, S., Bos-Burgering, L., Bradley, C., Budiyono, Y., Buytaert, W., Capewell, L., Carlson, H., Cavus, Y., Couasnon, A., Coxon, G., Daliakopoulos, I., de Ruiter, M. C., Delus, C., Erfurt, M., Esposito, G., François, D., Frappart, F., Freer, J., Frolova, N., Gain, A. K., Grillakis, M., Grima, J. O., Guzmán, D. A., Huning, L. S., Ionita, M., Kharlamov, M., Khoi, D. N., Kieboom, N., Kireeva, M., Koutroulis, A., Lavado-Casimiro, W., Li, H.-Y., LLasat, M. C., Macdonald, D., Mård, J., Mathew-Richards, H., McKenzie, A., Mejia, A., Mendiondo, E. M., Mens, M., Mobini, S., Mohor, G. S., Nagavciuc, V., Ngo-Duc, T., Thao Nguyen Huynh, T., Nhi, P. T. T., Petrucci, O., Nguyen, H. Q., Quintana-Seguí, P., Razavi, S., Ridolfi, E., Riegel, J., Sadik, M. S., Savelli, E., Sazonov, A., Sharma, S., Sörensen, J., Arguello Souza, F. A., Stahl, K., Steinhausen, M., Stoelzle, M., Szalińska, W., Tang, Q., Tian, F., Tokarczyk, T., Tovar, C., Tran, T. V. T., Van Huijgevoort, M. H. J., van Vliet, M. T. H., Vorogushyn, S., Wagener, T., Wang, Y., Wendt, D. E., Wickham, E., Yang, L., Zambrano-Bigiarini, M., Blöschl, G., and Di Baldassarre, G.: The challenge of unprecedented floods and droughts in risk management, Nature, 608, 80–86, https://doi.org/10.1038/s41586-022-04917-5, 2022.

Laumer, W., Andreu, L., Helle, G., Schleser, G. H., Wieloch, T., and Wissel, H.: A novel approach for the homogenization of cellulose to use micro-amounts for stable isotope analyses, Rapid Commun. Mass Spectrom., 23, 1934–1940, 2009.

Leavitt, S. W.: Tree-ring C–H–O isotope variability and sampling, Sci. Total Environ., 408, 5244–5253, https://doi.org/10.1016/j.scitotenv.2010.07.057, 2010.

Loader, N. J., Young, G. H. F., McCarroll, D., Davies, D., Miles, D., and Bronk Ramsey, C.: Summer precipitation for the England and Wales region, 1201–2000 CE, from stable oxygen isotopes in oak tree rings, J. Quaternary Sci., 35, 731–736, https://doi.org/10.1002/jqs.3226, 2020.

McCarroll, D. and Loader, N. J.: Stable isotopes in tree rings, Quaternary Sci. Rev., 23, 771–801, https://doi.org/10.1016/j.quascirev.2003.06.017, 2004.

Nagavciuc, V., Roibu, C.-C., Ionita, M., Mursa, A., Cotos, M.-G., and Popa, I.: Different climate response of three tree ring proxies of Pinus sylvestris from the Eastern Carpathians, Romania, Dendrochronologia, 54, 56–63, https://doi.org/10.1016/j.dendro.2019.02.007, 2019a.

Nagavciuc, V., Ionita, M., Perşoiu, A., Popa, I., Loader, N. J. N. J., and McCarroll, D.: Stable oxygen isotopes in Romanian oak tree rings record summer droughts and associated large-scale circulation patterns over Europe, Clim. Dynam., 52, 6557–6568, https://doi.org/10.1007/s00382-018-4530-7, 2019b.

Nagavciuc, V., Kern, Z., Ionita, M., Hartl, C., Konter, O., Esper, J., and Popa, I.: Climate signals in carbon and oxygen isotope ratios of Pinus cembra tree-ring cellulose from Călimani Mountains, Romania, Int. J. Climatol., 40, 2539–2556, https://doi.org/10.1002/joc.6349, 2020.

Nagavciuc, V., Ionita, M., Kern, Z., McCarroll, D., and Popa, I.: A $\sim$ 700 years perspective on the 21st century drying in the eastern part of Europe based on δ18O in tree ring cellulose, Commun. Earth Environ., 3, 277, https://doi.org/10.1038/s43247-022-00605-4, 2022a.

Nagavciuc, V., Scholz, P., and Ionita, M.: Hotspots for warm and dry summers in Romania, Nat. Hazards Earth Syst. Sci., 22, 1347–1369, https://doi.org/10.5194/nhess-22-1347-2022, 2022b.

Nagavciuc, V., Roibu, C.-C., Mursa, A., Ştirbu, M.-I., Popa, I., and Ionita, M.: The first tree-ring reconstrruction of streamflow variability over the last $\sim$ 250 years in the Lower Danube, J. Hydrol., 617, 129150, https://doi.org/10.1016/j.jhydrol.2023.129150, 2023.

Nagavciuc, V., Michel, S. L. L., Balting, D. F., Helle, G., Freund, M., Schleser, G. H., Steger, D. N., Lohmann, G., and Ionita, M.: A past and present perspective on the European summer vapor pressure deficit, Clim. Past, 20, 573–595, https://doi.org/10.5194/cp-20-573-2024, 2024a.

Nagavciuc, V., Helle, G., Rădoane, M., Roibu, C.-C., Cotos, M.-G., and Ionita, M.: A long-term drought reconstruction (August SPEI9) based on oxygen isotope tree ring data for central and eastern parts of Europe (Romania), Zenodo [data set], https://doi.org/10.5281/zenodo.14536886, 2024b.

Paul, D., Skrzypek, G., and Fórizs, I.: Normalization of measured stable isotopic compositions to isotope reference scales – a review, Rapid Commun. Mass Spectrom., 21, 3006–3014, https://doi.org/10.1002/rcm.3185, 2007.

Penman, H. L.: Natural evaporation from open water, bare soil and grass, P. Roy. Soc. Lond. A. Mat., 193, 120–145, https://doi.org/10.1098/rspa.1948.0037, 1948.

Pfister, C.: Wetternachhersage, 500 Jahre Klimavariationen und Naturkatastrophen (1496–1995), Verlag Paul Haupt, Bern Stuttgart Wien, 301 pp., 1999.

Pumijumnong, N., Bräuning, A., Sano, M., Nakatsuka, T., Muangsong, C., and Buajan, S.: A 338-year tree-ring oxygen isotope record from Thai teak captures the variations in the Asian summer monsoon system, Sci. Rep., 10, 8966, https://doi.org/10.1038/s41598-020-66001-0, 2020.

Rinne, K. T., Boettger, T., Loader, N. J., Robertson, I., Switsur, V. R., and Waterhouse, J. S.: On the purification of α-cellulose from resinous wood for stable isotope (H, C and O) analysis, Chem. Geol., 222, 75–82, https://doi.org/10.1016/j.chemgeo.2005.06.010, 2005.

Robertson, I., Field, E. M., Heaton, T. H. E., Pilcher, J. R., Pollard, A. M., Switsur, V. R., Waterhouse, J. S., Frenzel, B., Stauffer, B., and Weiss, M. M.: Problems of stable isotopes in tree-rings, lake sediments and peat-bogs as climatic evidence for the Holocene, Paläoklima, European Science Foundation, Strasbourg, 141–155, ISBN 3437308173 9783437308178, 1995.

Roden, J., Lin, G., and Ehleringer, J. R.: A mechanistic model for interpretation of hydrogen and oxygen isotope ratios in tree-ring cellulose, Geochim. Cosmochim. Ac., 64, 21–35, 2000.

Roibu, C.-C., Nagavciuc, V., Ionita, M., Popa, I., Horodnic, S.-A., Mursa, A., and Büntgen, U.: A tree ring-based hydroclimate reconstruction for eastern Europe reveals large-scale teleconnection patterns, Clim. Dynam., 59, 2979–2994, https://doi.org/10.1007/s00382-022-06255-8, 2022.

Sandu, I., Pescaru, V. I., and Poiana, I.: Clima Romaniei, Bucureşti: Editura Academiei Române, 365 pp., ISBN 973-27-1674-8, 2008 (in Romanian).

Saurer, M., Kress, A., Leuenberger, M., Rinne, K. T., Treydte, K. S., and Siegwolf, R. T. W.: Influence of atmospheric circulation patterns on the oxygen isotope ratio of tree rings in the Alpine region, J. Geophys. Res.-Atmos., 117, D05118, https://doi.org/10.1029/2011JD016861, 2012.

Schweingruber, F. H.: Tree Rings Basics and Applications of Dendrochronology, 276 pp., https://doi.org/10.1007/978-94-009-1273-1, 1988.

Sharp, Z.: Principles of Stable Isotope Geochemistry, Pearson Pr., edited by: Rapp, C., American Library Association, New Jersey, 344 pp., https://doi.org/10.5860/choice.44-6251, 2007.

Siegwolf, R. T. W., Brooks, J. R., Roden, J., and Saurer, M. (Eds.): Stable Isotopes in Tree Rings Inferring Physiological, Climatic and Environmental Responses, Series Tit., Springer, Cham, Switzerland, 773 pp., https://doi.org/10.1007/978-3-030-92698-4, 2022.

Van der Sleen, P., Groenendijk, P., and Zuidema, P. A.: Tree-ring δ^{18}O in African mahogany (Entandrophragma utile) records regional precipitation and can be used for climate reconstructions, Global Planet. Change, 127, 58–66, https://doi.org/10.1016/j.gloplacha.2015.01.014, 2015.

Van Loon, A. F., Kchouk, S., Matanó, A., Tootoonchi, F., Alvarez-Garreton, C., Hassaballah, K. E. A., Wu, M., Wens, M. L. K., Shyrokaya, A., Ridolfi, E., Biella, R., Nagavciuc, V., Barendrecht, M. H., Bastos, A., Cavalcante, L., de Vries, F. T., Garcia, M., Mård, J., Streefkerk, I. N., Teutschbein, C., Tootoonchi, R., Weesie, R., Aich, V., Boisier, J. P., Di Baldassarre, G., Du, Y., Galleguillos, M., Garreaud, R., Ionita, M., Khatami, S., Koehler, J. K. L., Luce, C. H., Maskey, S., Mendoza, H. D., Mwangi, M. N., Pechlivanidis, I. G., Ribeiro Neto, G. G., Roy, T., Stefanski, R., Trambauer, P., Koebele, E. A., Vico, G., and Werner, M.: Review article: Drought as a continuum – memory effects in interlinked hydrological, ecological, and social systems, Nat. Hazards Earth Syst. Sci., 24, 3173–3205, https://doi.org/10.5194/nhess-24-3173-2024, 2024.

Teodoreanu, E.: În căutarea timpului trecut Schiă de climatologie istorică, Editura Paodeia, Bucuresti, 363 pp., ISBN 9786067482140, 2017.

Topor, N.: Anii ploioşi şi secetoşi din Republica Populară Romînă, C.S.A Institutul Meteorologic, Bucureşti, 1963.

Yang, X., Zeng, G., Zhang, S., Iyakaremye, V., Shen, C., Wang, W.-C., and Chen, D.: Phase-Locked Rossby Wave-4 Pattern Dominates the 2022-Like Concurrent Heat Extremes Across the Northern Hemisphere, Geophys. Res. Lett., 51, e2023GL107106, https://doi.org/10.1029/2023GL107106, 2024.

Young, G. H. F., Loader, N. J., McCarroll, D., Bale, R. J., Demmler, J. C., Miles, D., Nayling, N. T., Rinne, K. T., Robertson, I., Watts, C., and Whitney, M.: Oxygen stable isotope ratios from British oak tree-rings provide a strong and consistent record of past changes in summer rainfall, Clim. Dynam., 45, 3609–3622, https://doi.org/10.1007/s00382-015-2559-4, 2015.

Zang, C. and Biondi, F.: Treeclim: An R package for the numerical calibration of proxy-climate relationships, Ecography, 38, 431–436, https://doi.org/10.1111/ecog.01335, 2015.